



## Performance Assessment of Steel Eccentrically Braced Frames Equipped with Cast Steel Replaceable Modular Yielding Links through Pseudo-dynamic Hybrid Simulations

Pedram Mortazavi<sup>1\*</sup>, Oh-Sung Kwon<sup>2</sup>, and Constantin Christopoulos<sup>3</sup>

<sup>1</sup>PhD Candidate, Department of Civil and Mineral Engineering, University of Toronto, Toronto, ON, Canada

<sup>2</sup>Professor, Department of Civil and Mineral Engineering, University of Toronto, Toronto, ON, Canada

<sup>3</sup>Professor, Director of the Structural Testing Facilities, and Canada Research Chair in Seismic Resilience of Infrastructure, Department of Civil and Mineral Engineering, University of Toronto, Toronto, ON, Canada

\*[pedram.mortazavi@mail.utoronto.ca](mailto:pedram.mortazavi@mail.utoronto.ca) (Corresponding Author)

### ABSTRACT

Cast steel replaceable modular yielding links were previously proposed for use in eccentrically braced frames (EBFs). Experimental validations of cast steel links demonstrated a stable hysteretic response for the proposed links with highly increased ductility and ultra-low cycle fatigue life when compared to conventional fabricated links. In addition, the proposed cast steel links simplify the design process for EBFs with modular links by eliminating iterations needed for meeting the link design rotation limit. Further, they promote modular construction and simplify post-earthquake repairs. As the next step in this development, the response of EBF building structures designed with cast steel replaceable yielding links under real earthquake excitations was studied. This paper presents pseudo-dynamic hybrid simulations on two prototype EBF structures equipped with cast steel replaceable modular yielding links, designed according to ASCE 7-16 provisions. A four-story structure was designed such that the yielding link would experience no axial loads. In addition, a two-story structure was designed such that the yielding link on the second floor would experience large axial loads during its response. In hybrid simulations on the four-story structure, the response of the first floor yielding link was physically captured in the laboratory, while the response of the rest of the structure was captured numerically in OpenSees. For the two-story structure, the response of the second floor yielding link was captured physically, while the response of the rest of the structure was obtained numerically in OpenSees. The hybrid simulation framework including the test setups, the substructuring strategy, the communication scheme, and the modelling approach for capturing the response of cast steel links are presented. These experiments serve as benchmark test results, which can be used for better calibration of numerical models. Each building structure is subjected to three MCE-level earthquakes. The experimental results demonstrate that cast steel replaceable modular yielding links can sustain large-deformations and provide stable energy dissipation during real earthquakes.

Keywords: Steel Casting, Eccentrically Braced Frames, Hybrid Simulations, Hysteretic Yielding Dampers, Large-Scale Testing

### INTRODUCTION

#### Background

Eccentrically braced frames (EBFs) were first proposed as a seismic force resisting system (SFRS) in Japan [1] and were then studied in the United States [2-10]. EBFs combine the advantages of Special Moment Resisting Frames (SMRFs) and Special Concentrically Braced Frames (SCBFs). While their energy dissipation capacity is comparable to SMRFs, they can provide the structure with a desirable lateral stiffness, which is achieved through the use of diagonal braces in EBFs. EBFs are also favored by architects, compared to SCBFs, as they allow for more and larger openings within the SFRS. The energy dissipation of EBFs is achieved through yielding of a portion of the floor beam between the two braces, which is referred to as the yielding link. Wide-flange steel sections (W-Sections) are the most commonly used section for design and detailing of yielding links in EBFs. However, researchers have considered the use of other sections as well, such as hollow box sections [11] and double channel sections [12]. Built-up sections have also been considered for the design of yielding links in EBFs [13]. Yielding links can be designed as shear critical links, flexural links, or intermediate links, depending on their yielding length ( $e_y$ ), nominal shear plastic capacity ( $V_p$ ), and their plastic moment capacity ( $M_p$ ). Shear-critical links are the preferable design, as they

facilitate simultaneous yielding across the web by using welded web stiffeners. As such design codes [14-15] provide a rotation limit of 0.08 radians for shear-critical links, whereas the rotation limit for flexural links is 0.02 radians.

### **Replaceable Yielding Links**

To simplify the design, construction, and post-earthquake repairs of EBFs, replaceable links were proposed about a decade ago [12]. Replaceable links decouple the yielding link from the beam outside of the link, allowing for preventing the beam outside of the link from yielding. In addition, use of replaceable links promotes modular construction and a more seamless post-earthquake repair process in EBFs. Therefore, replaceable links were received well by the engineering community and were used in the rebuilding of Christchurch as well [16]. However, replaceable links require stringent welding requirements and have similar limit states as conventional links. They also have the same rotation limit of 0.08 radians.

### **Cast Steel Replaceable Modular Yielding Links**

The freedom of geometry offered by steel casting technology enables engineers to propose custom-designed shapes for an improved structural performance, which may not be feasible with conventional welded fabrication. In addition to geometric optimization, steel castings allow for an optimized performance on a material level through heat treatments and quality control. Therefore, steel casting is a well suited material for design and fabrication of energy dissipative hysteretic dampers [17-19]. In addition, steel casting reduces residual stresses and stress concentrations [20] and is a more economical option for fabrication of complex and mass-produced shapes [21].

In order to address the limitations associated with the design of EBFs and to further improve their performance, cast steel replaceable modular yielding links were recently developed and experimentally validated in a series of studies [22-26]. Cast steel yielding links are illustrated in Figure 1. In the first design of cast steel links [23], nine links were designed, which are shown in Figure 1. In a subsequent study [24], additional cast steel links were designed and validated which were shorter in length but had more consistent ductility capacity among the different links. As can be observed in Figure 1, cast steel replaceable yielding links consist of four primary regions: (1) The tapered hollow box yielding portion, (2) The elastic segment which transfers the shears, moments, and axial loads, (3) The integral cast endplate, and (4) The transition fillets. Each link is referred to as EBF, followed by a number, which shows the  $V_p$  of that link size in *kips*. The link  $V_p$  is also shown in *kN* in brackets.  $V_p$  refers to the shear load at which the entire yielding region of links have reached full plasticity. Experimental validation of cast steel yielding links [23-27] has demonstrated an excellent performance for the proposed links in terms of ductility and ULCF life, being able to sustain rotations as high as 0.21 radians.

### **Paper Content**

This study presents pseudo-dynamic hybrid simulations on two prototype building structures designed with EBFs that are equipped with the proposed cast steel replaceable modular yielding links. The hybrid simulations are primarily intended to study the global performance of EBF building structures equipped with cast steel replaceable modular yielding links under real earthquake ground motion records. In addition, the methodology presented in this paper can be used as a framework for performing pseudo-dynamic hybrid simulations on EBFs, while capturing the response of the yielding link physically with or without axial loading, with a single degree of freedom (SDOF) control system. Results from the hybrid simulations could also be used as high-fidelity system-level benchmark test results for the calibration of numerical models for capturing the response of EBFs with cast steel yielding links. These benchmark test results can also assist with proposing new loading protocols which are better able to capture the intricacies of the hysteretic response of structural systems, which may not be manifested well under incremental reversed-cyclic experimental results. Previous studies have proposed ways to improve loading protocols [27], and some studies have even proposed more specific loading protocols for structural components and the type of analysis performed. For instance, Suzuki and Lignos [28] have proposed collapse-consistent loading protocols for column members. High-fidelity benchmark test results will further assist researchers with developing such loading protocols. Previous studies have also presented the challenges associated with calibrating the numerical models to reversed-cyclic test results and provided benchmark test results for different structural systems [19,29-30]. The paper first presents the prototype structures and the ground motions that are used in the hybrid simulations. Next, the hybrid simulation framework including the experimental test setups, the numerical models, and the communication scheme is presented. Selected hybrid simulation test results are then presented and discussed.

## **PROTOTYPE BUILDINGS AND GROUND MOTION RECORDS**

### **Four-Story Prototype Structure**

The four-story prototype EBF structure is an office building of normal importance located in downtown Los Angeles, on site class 'C'. The building plan and an elevation of the building along gridline 1 are shown in Figure 2. The building's SFRSs are formed by SMRFs in the north-south direction, and by EBFs in the east-west direction. The structure is designed and analyzed

in the east-west direction, in the present study. All structural members were designed as per the provisions of ASCE 7-16 [31], AISC 360-16 [32], and AISC 341-16 [33]

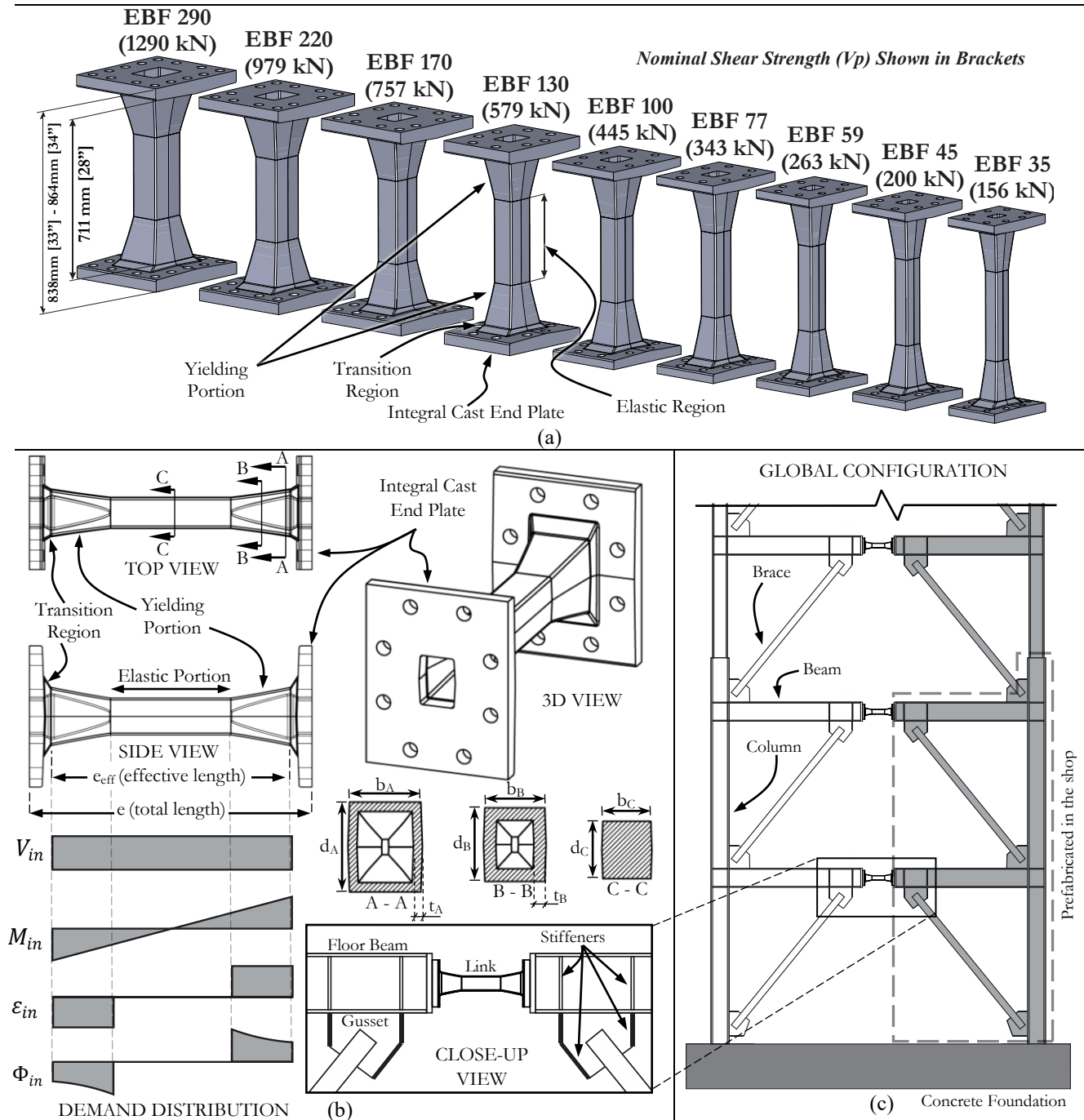


Figure 1. Cast Steel Replaceable Modular Yielding Links: (a) Sizes, (b) Details and Mechanics, and (c) Global Illustration

The selected cast steel yielding link sizes on floors one to four were EBF100, EBF100, EBF77, and EBF45, respectively. EBF columns were sized as W310×79 members below the splice, while W310×45 sections were used for columns above the splice. Braces on the first and second floors were W200×71 members, and braces on the third and fourth floors were W200×52 sections. The floor beams within the EBF from stories one to four were selected as W410×67, W410×60, W360×51, and W250×39 sections, respectively. The steel grade for all structural elements other than the yielding links was ASTM A572 Grade 50. Out of the eight EBFs in the east-west direction of the structure, as shown in Figure 2, one of the EBFs was studied in the hybrid simulations. This approach is justified given that the response of the eight EBFs is identical in the absence of accidental torsion. The building's fundamental period was 0.5 seconds. The structure's seismic weight for floors one to four

was determined to be 4321 kN, 4308 kN, 4292 kN, and 3633 kN, respectively, for a total seismic weight of 16554 kN. The design period ( $T_d$ ) was taken as 0.5 seconds. Spectral acceleration for the first mode was 1.3g, where g is the gravitational constant. The base shear was determined using the response spectrum analysis (RSA) method and was scaled up to match 100% of the base shear from the equivalent static force procedure (ESFP), which was 2700 kN.

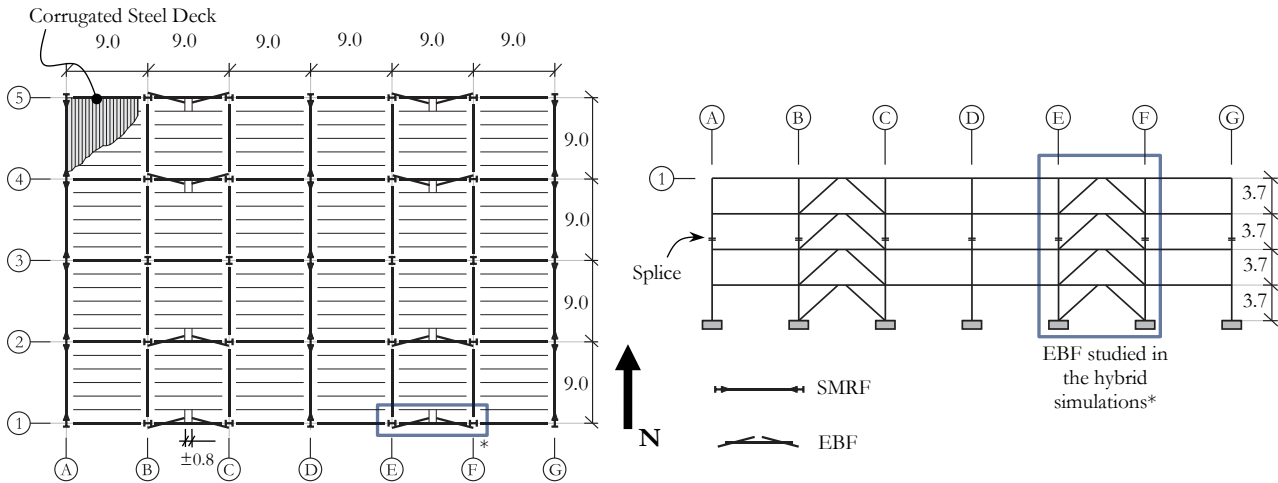


Figure 2. Illustration of the Prototype Four-Story EBF Office Building (all dimensions in meters)

### Two-Story Prototype Structure

The two-story prototype building is an industrial compound located in downtown Los Angeles. The first floor and the roof level plans are shown in Figures 3 (a) and 3 (b). The building's top view and an elevation along gridline 1 are also shown in Figures 3 (c) and (d). The SFRSs of the building are formed by SCBFs in the north-south direction, and by EBFs in the east-west direction. The area on the ground floor between gridlines A to D, and gridlines H to K, is used as storage space. The remaining enclosed spaces on the first floor are used as office space. The first floor consists of two separated areas to provide a large open space in order to facilitate truck access to the industrial compound. In addition, there is a setback in the south portion of the first-floor plan (within gridlines A – H and 1 – 2) to allow space for visitor's parking. A similar open space between gridlines D – K and 9 – 10 is allocated to staff parking, which can be seen in Figure 3 (c). There is also a setback along the building's height as the roof plan is smaller than the first-floor plan, as shown in Figure 3 (d). In order to accommodate the larger 18-meter spans over the area designated for truck access, deep gravity trusses are used at the roof level to carry the gravity loads to the columns. Typical floor height is 3,543 mm. The typical floor span in the east-west direction, other than the area for truck access, is 9 meters. In the north-south direction the span lengths range from 6 meters to 9 meters.

All members were designed as per the provisions of ASCE 7-16 [31], AISC 360-16 [32], and AISC 341-16 [33]. The yielding links on the first floor and roof level were EBF100s and EBF77s, respectively. All EBF columns were designed with W310×52 sections. The EBF floor beams were designed with W360×64 and W360×51, on the first floor and the roof level, respectively. The braces in the EBFs on the ground and the first floor were sized with W200×71 and W200×52 sections, respectively. In the final design iteration, the total seismic weight of the building was determined to be 26880 kN, with 13510 kN at the first floor and 13370 kN at the roof level. The fundamental period the structure in the direction of interest was determined to be 0.335 seconds, obtained from a 3D analytical model.  $T_d$  was taken as 0.335 seconds. The building's spectral acceleration for the first mode was determined to be 1.57g. The base shear from the RSA was scaled up to match 100% of the base shear from the ESFP, which was 5277 kN.

Given the building's geometry, the first floor yielding links experience no axial loads during their seismic response. However, the yielding links at the roof level will experience axial loads in conjunction with shear and bending moments. In addition, at any given time during the response, half of the roof yielding links on one side of the centerline will experience axial compression, while the other half will be in tension. Therefore, for studying the seismic response of the structure, at least two EBFs must be included in the numerical model, including one EBF with its top floor link in compression and one with its top floor link in tension. It can be shown [34,35] that the level of axial load in the roof level yielding links is around  $1.11 V_{Link}$  where  $V_{Link}$  is the shear force in the yielding link at any given time.

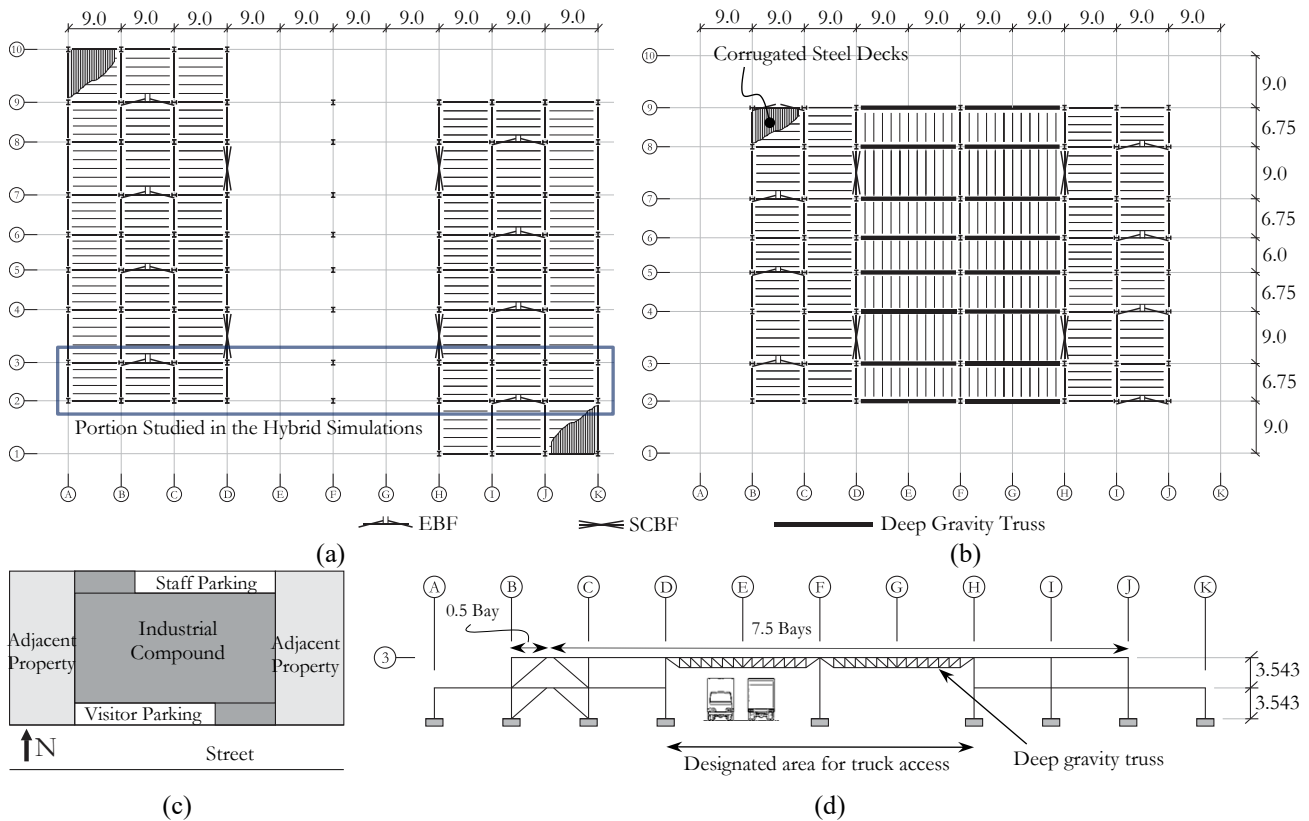


Figure 3. Illustration of the Prototype Two-Story Industrial Compound with Steel EBFs (all dimensions in meters): (a) First Floor Plan, (b) Roof Plan, (c) Top View, and (d) Elevation along Gridline 3

### Seismic Hazard and Selected Records

The records used in the hybrid simulations were selected from a suite of forty ground motions from the Pacific Earthquake Engineering Research Centre (PEER) ground motion database [36] and scaled to match the uniform hazard spectrum of downtown Los Angeles. The selected records are shown in Table 1. Additional details regarding the ground motions are provided by [34].

Table 1. Ground Motion Records Used in the Hybrid Simulations

Record No.	Scale factor	Earthquake	Station	Year	M	R (km)	$V_{s30}$ (m/s)	Pulse period (s)
1	3.370	"Northridge-01"	" N Hollywood - Coldwater Can"	1994	6.7	12.5	327	-
2-1	1.970	"L-Aquila Italy"	" L'Aquila - V. Aterno - Centro Valle"	2009	6.3	6.27	475	1.071
2-2*	1.160	"L-Aquila Italy"	" L'Aquila - V. Aterno - Centro Valle"	2009	6.3	6.27	475	1.071
3	3.075	"Loma-Prieta"	"Gilroy Array #3"	1989	6.9	12.80	350	2.639
4	1.845	"Kobe-Japan"	"Nishi-Akashi"	1995	6.9	7.08	609	-

### HYBRID SIMULATION FRAMEWORK

#### Numerical Modelling Approach

The numerical model that was used for modelling the cast steel replaceable yielding links is shown in Figure 4. The yielding links were modelled using a series of fibre sections and nonlinear *forceBeamColumn* elements in OpenSees, which can capture the interaction between bending moments and axial loads. Each fibre section is also aggregated with an elastic section, capturing the elastic shear deformation. The steel material was modelled using the Giuffrè–Menegotto–Pinto uniaxial stress–strain relationship (Steel02 material) in OpenSees. The yield stress ( $F_y$ ) of the material was taken as 330 MPa, and the modulus of elasticity ( $E$ ) was taken as 200000 MPa from coupon test results. Additional parameters affecting the hysteretic response including the post-yield stiffness ( $b$ ),  $R_o$ ,  $cR1$ ,  $cR2$ ,  $a_1$ ,  $a_2$ ,  $a_3$ , and  $a_4$  parameters were taken as 0.003, 20, 0.92, 0.15, 0.025, 1.0, 0.025, and 1.0, respectively. The results of the calibration of the numerical model to reversed cyclic test results on cast steel links [24] is also provided in Figure 4.

The global modelling approach is shown in Figure 5, for the four-story and the two-story EBF structures. The numerical models were developed in OpenSees. Given the symmetry of the structures, two-dimensional models were used. The beams, columns,

and braces were modelled using *beamWithHinges* elements using fibre sections. The steel material for other elements outside of the links was modelled using the Steel02 material with a 2% post-yield stiffness. The yield stress of the steel elements was specified as 345 MPa. The parameters  $R0$ ,  $cR1$ , and  $cR2$  were taken as 18, 0.925, and 0.15, respectively. A leaning column was modelled in order to capture the P-Delta effects in the structure. The weight of the structure associated with the frames in the numerical model was applied to the leaning column at each floor. In addition, the floor nodes were constrained to the nodes on the leaning columns in order to emulate a rigid diaphragm constraint. For the four-story structure, the seismic mass was equally lumped at two nodes of the EBF, at each floor. The same approach was adopted for the first floor of the two-story structure. At the roof level, however, the seismic mass associated with 7.5 bays was lumped to one side, while the seismic mass associated with half a bay was lumped to the other side in order to capture the imbalanced inertia load as shown in Figure 3 (d). The periods of the first two modes of vibration for the four-story structure were found to be 0.534 s and 0.211 s. For the two-story structure these values were found to be 0.383 s and 0.154 s. An inherent viscous damping of 3% was assumed in the first two modes in each model. Additional details regarding the numerical models can be found in [34].

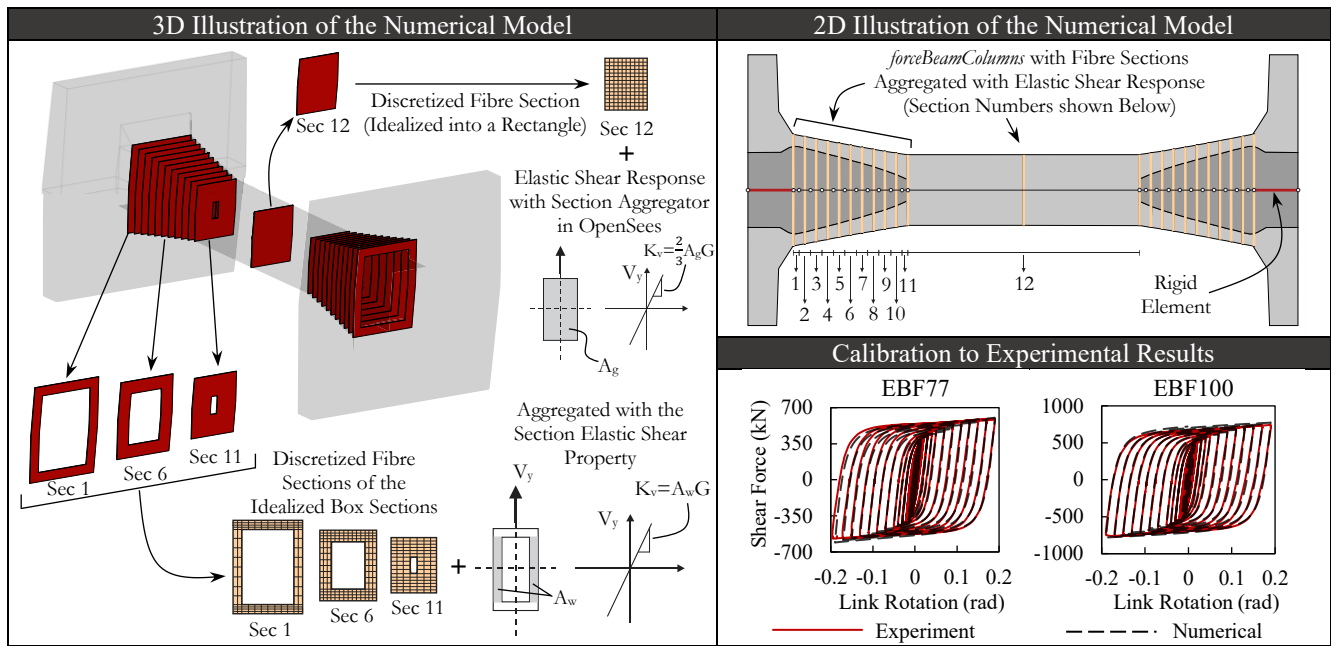


Figure 4. Numerical Model for Capturing the Response of Cast Steel Replaceable Modular Yielding Links

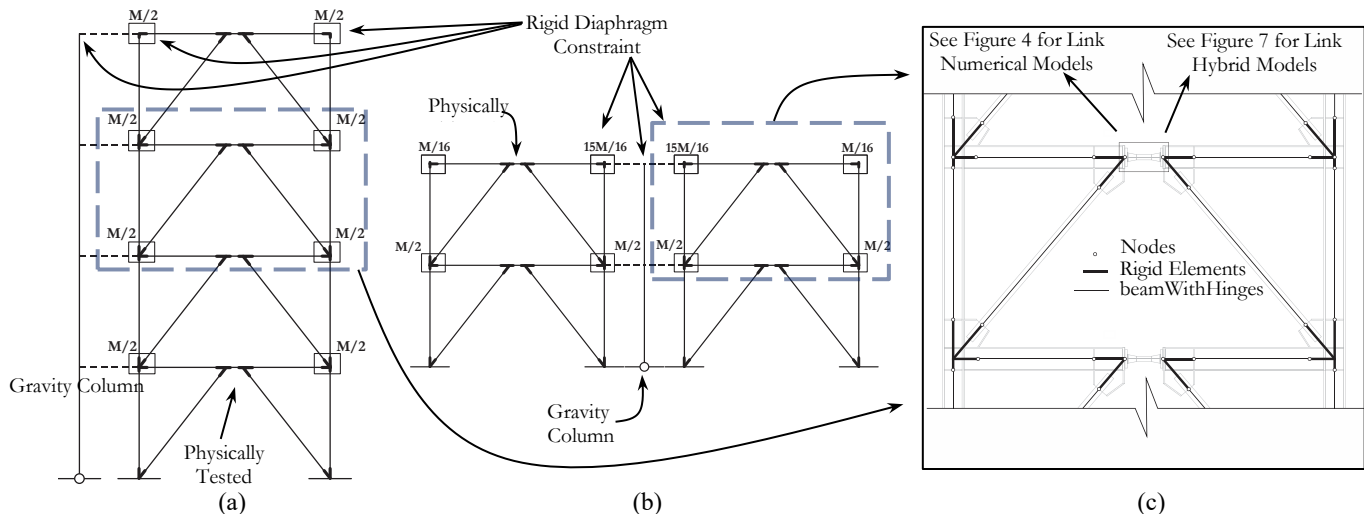


Figure 5. Numerical Model for Capturing the Global Response of EBFs

### Experimental Test Setups

The experimental setups used to capture the physical response of the specimens are shown in Figure 6. A pure shear test setup was used to capture the response of the first floor yielding link in hybrid simulations on the four-story EBF, which is shown in Figure 6 (a). The pure shear test setup was chosen for these experiments, as it does not impose a notable axial load on the

yielding link. A one-story frame setup was used to capture the response of one of the yielding links at the roof level in hybrid simulations on the two-story EBF structure. The one-story frame setup was designed such that the ratio of yielding link axial load ( $P_{Link}$ ) to the link's shear load ( $V_{Link}$ ) was around 1.11 during the experiments, similar to the case in the two-story structure. Additional details regarding the experimental test setups, instrumentations, and relevant assumptions can be found in previous studies [23,34].

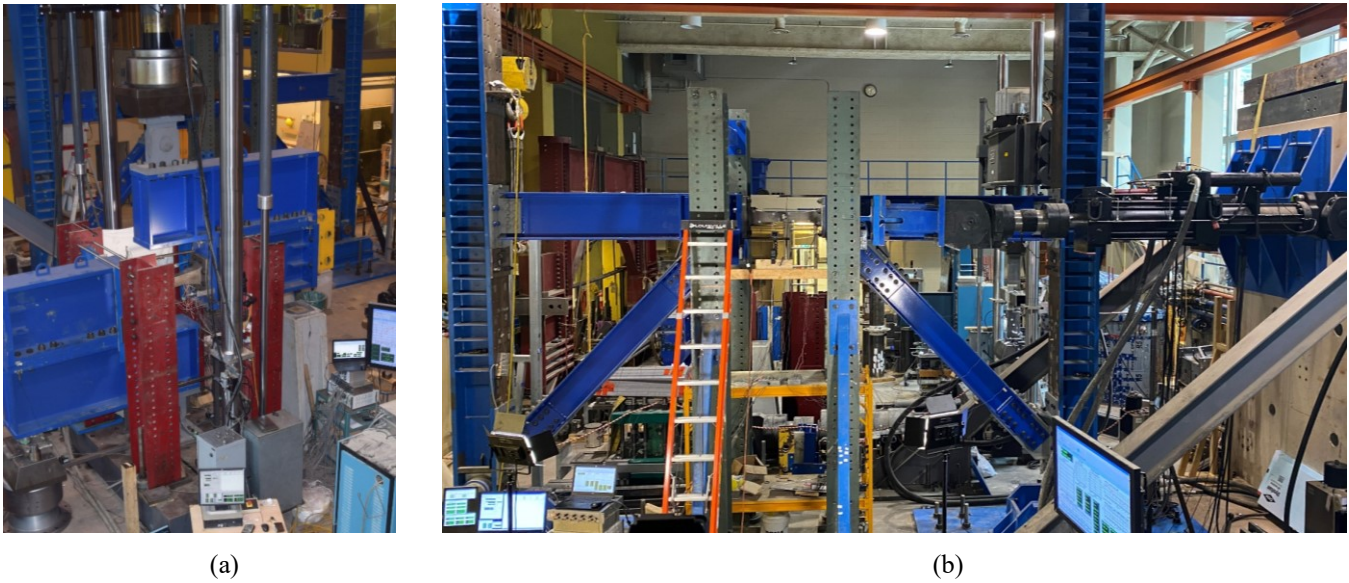


Figure 6. Experimental Setups: (a) Component-Level Test Setup, and (b) System-Level Test Setup

### Substructuring Strategy

The substructuring strategies used in the hybrid simulations are shown in Figure 7. In hybrid simulations on the four-story EBF, the response of the first-floor link was physically captured in the laboratory in the pure shear test setup, while the response of the rest of the structure was modelled numerically in OpenSees. In hybrid simulations on the two-story EBF the response of one of the yielding links at the roof level was physically captured in the one-story frame setup, while the response of the remainder of the structure was modelled numerically in OpenSees. At the location of the yielding link, the response of which was physically captured in the laboratory, a set of rigid elements were modelled as shown in Figure 7 in order to facilitate capturing the response of the yielding link in a SDOF control system.

### Specimens

The cast steel yielding links that were tested in the hybrid simulations are shown in Table 2, along with their specifications. The parameters given in Table 2, for each cast steel yielding link, are shown in Figure 1. In addition, Table 2 provides the elastic stiffness ( $K_{EI}$ ) for each yielding links. The EBF100 link was tested in hybrid simulations on the four-story structure as the first floor yielding link. In hybrid simulations on the two-story structure, an EBF77 was tested as the roof yielding link.

Table 2. Cast Steel Links Tested in the Hybrid Simulations

Link Size	$b_A$	$d_A$	$t_A$	$b_C$	$d_C$	$K_{EI}$	$V_p$	$e$	$e_{eff}$
EBF77	124.9	158.7	15.6	82.2	100.7	73.2	342	838.2	711.2
EBF100	136.3	173.2	17.0	89.5	109.5	100.9	444	838.2	711.2

All values reported in kN and mm

### Integration Scheme

In the OpenSees model, a non-iterative Alpha-OS integration scheme [37] with a linear algorithm was utilized to solve the system of equations of motion. This approach employs the Alpha-modified Newmark scheme to effectively damp spurious oscillations resulting from the numerical model. The time step for all hybrid simulations was set at 0.01 s. Before conducting the hybrid simulations, purely numerical simulations were carried out on the reference structures using different time step sizes, and a 0.01 s integration time step was determined to be sufficiently accurate.

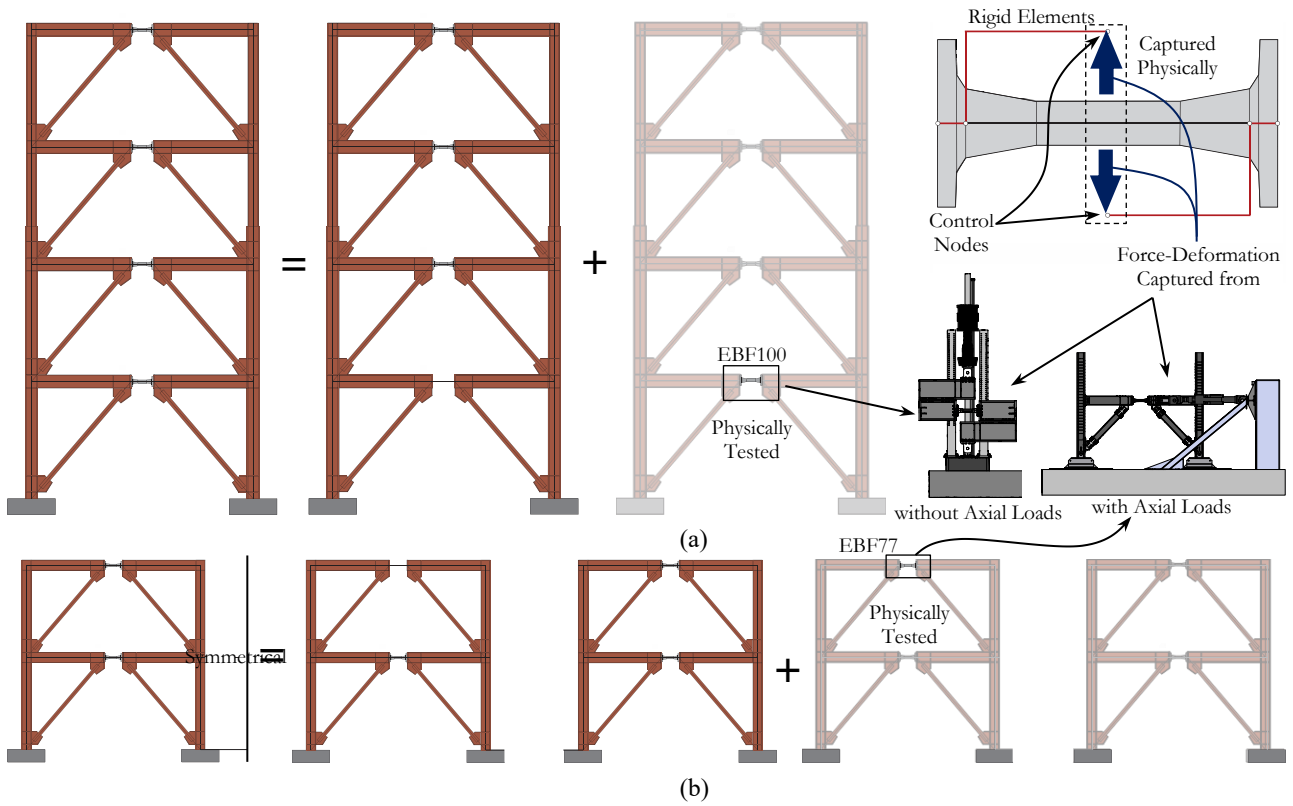


Figure 7. Substructuring Strategy (a) Four-Story EBF Building, and (b) Two-Story EBF Building

### Data Communications

The data communications scheme for the hybrid simulations on the four-story reference structure is shown in Figure 8. The data communications for hybrid simulations on the two-story structure is similar, but after the experiment's required coordinate transformations, which are presented in [34,35] in detail. Data communications are done using the University of Toronto Simulation Framework (UT-SIM), which is a generalized framework for distributed multiplatform simulations through network communications between numerical/experimental substructures [38-40]. The response of the yielding link on the first floor is captured using the *SubStructure* element within the UT-SIM, which facilitates data communications between the OpenSees model and the Network Interface for Actuator Controllers (NICON) [41,42], which is a program based in LabVIEW [43]. NICON establishes communications between the numerical model and the MTS actuator controllers [44]. Therefore, at any given step during the hybrid simulation displacement commands are communicated from the numerical model to the physical substructure. After the target displacement command is achieved through iterations, the measured force and displacement are fed back to the numerical model. Additional details regarding the data communications in hybrid simulations on the four-story EBF and data communications for hybrid simulations on the two-story EBF structure are provided by [34].

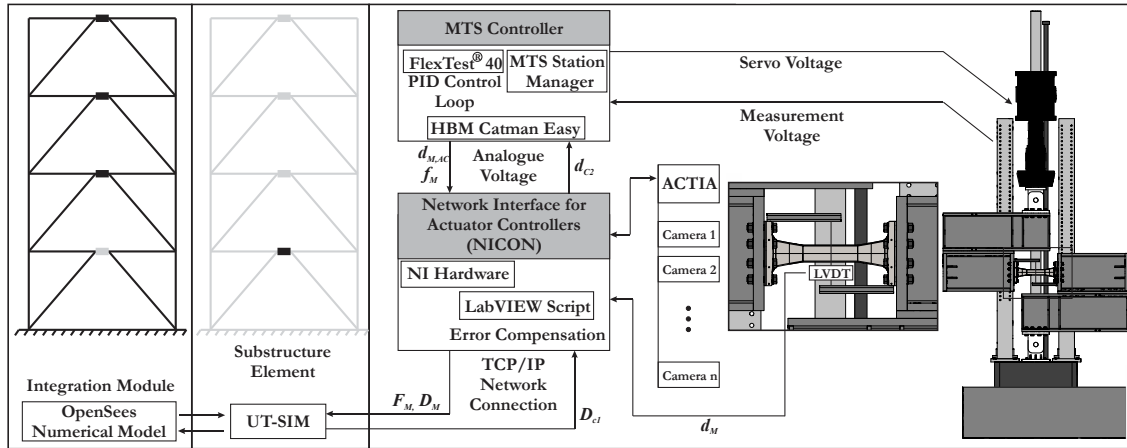


Figure 8. Data Communications in Hybrid Simulations on the Four-Story EBF

### Hybrid Simulation Cases

A total of six hybrid simulations were conducted. The first three simulations, labeled HS-1, HS-2, and HS-3, were carried out on the four-story EBF using records 2-2, 1, and 4. The other three simulations, referred to as HSF-4, HSF-5, and HSF-6, were performed on the two-story EBF using records 3, 1, and 2-1.

### SELECTED TEST RESULTS

#### Four-Story Reference Structure

Figure 9 shows the rotation response history of the first-floor link. Figure 9 (b) shows the transient and residual rotations of the yielding links throughout the height of the building. The pattern of drift response along the building's height was similar to the link rotations. However, the drift levels were much more moderate with maximum values not exceeding 1.5% in HS-3, and slightly above 1.0% in hybrid simulations HS-1 and HS-2. The hysteretic response of the first-floor link is also illustrated in Figure 9. The experimental results are also compared to results from the purely numerical simulations. Even though the residual drift levels were observed to be moderate, the link experienced significant residual rotations in experiments HS-1 and HS-3.

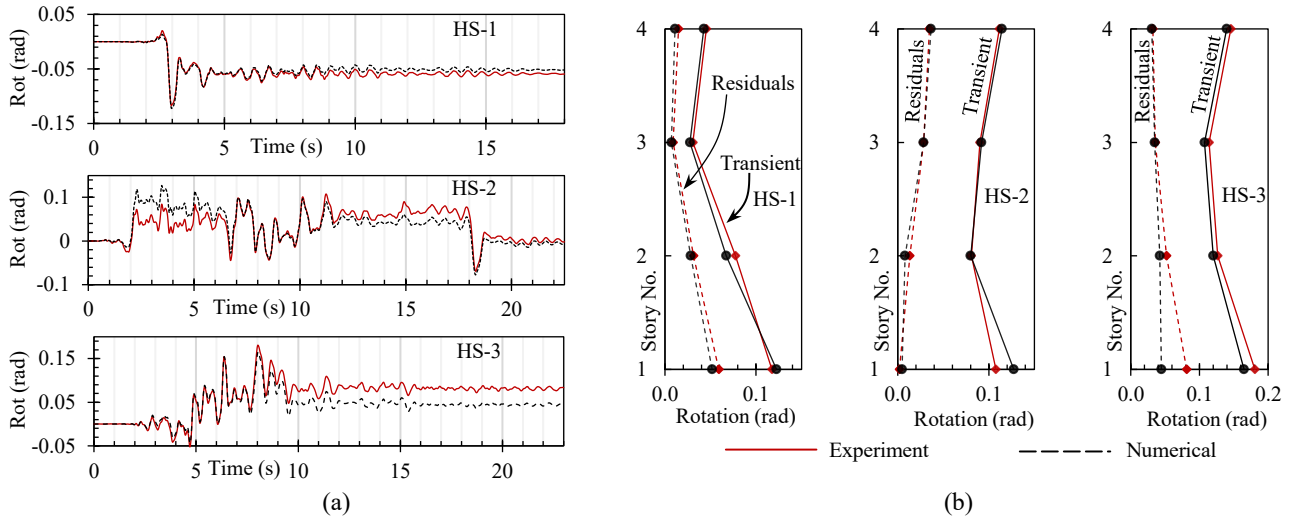


Figure 9. Link Rotation Response from Hybrid Simulations on the Four-Story Office Building: (a) Response History of the First Floor Link, and (b) Link Rotation Distribution over Height

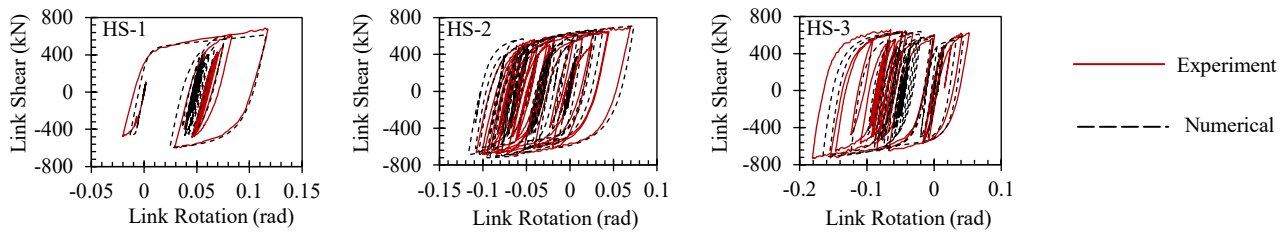


Figure 10: First-Floor Link Hysteretic Responses from Hybrid Simulations on the Four-Story Office Building

#### Two-Story Reference Structure

Results from hybrid simulations HSF-4, HSF-5, and HSF-6 are provided in Figures 11 (a) and 11 (b), in terms of the rotation response history of the roof level yielding link and the distribution of link rotations along the building height. The roof level link hysteretic response is presented in Figure 12. The experimental results are also compared to results from the purely numerical simulations. The drift levels in the two-story EBF also followed the same pattern as the link rotation response. The maximum drift values in hybrid simulations HSF-4, HSF-5, and HSF-6 were 1.5%, 1.3%, and 2.0%, respectively.

#### Performance of the Capacity Protected Elements

The performance of the secondary elements including beams, columns, and braces in the EBFs were studied in the hybrid simulations. Results from the hybrid simulations of a four-story reference EBF indicated that all beams, columns, and braces remained elastic throughout the three earthquakes, as they were designed to be capacity protected. However, in the case of a two-story reference EBF, while the braces remained elastic during all earthquakes, there was negligible yielding observed in the columns under the 2-2\* earthquake and moderate yielding observed in the EBF beams at the second floor. This was because the yielding links at the second floor were subjected to large axial loads, and current guidelines provided by AISC 2016 [33],

do not provide recommendations on estimating the increase in the yielding link's overstrength in EBFs when it is subjected to large axial tension loads.

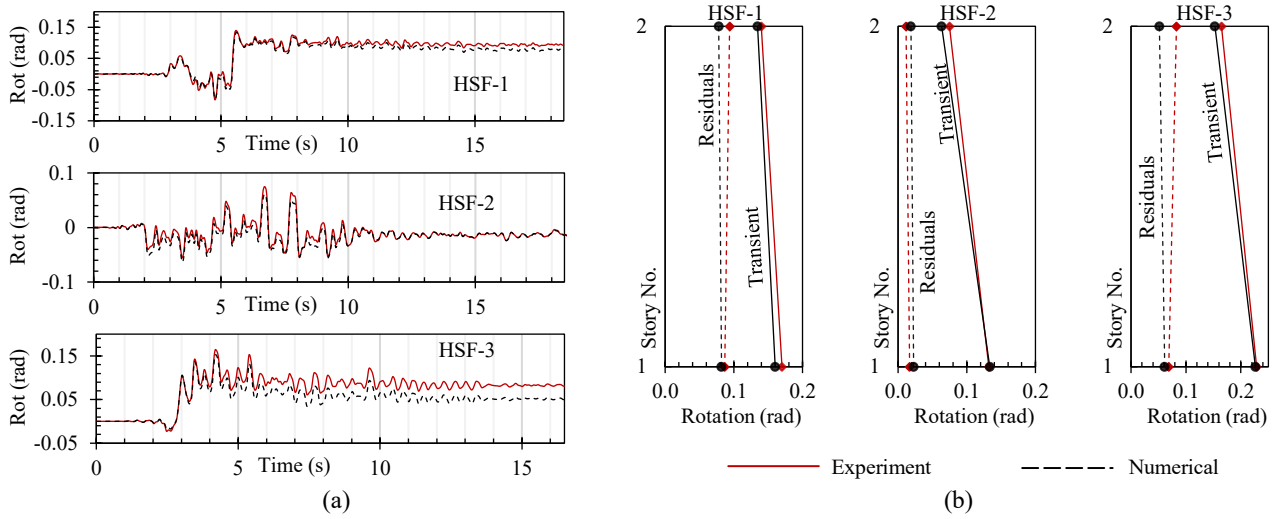


Figure 11. Link Rotation Response from Hybrid Simulations on the Two-Story Office Building: (a) Response History of the Second Floor Link, and (b) Link Rotation Distribution over Height

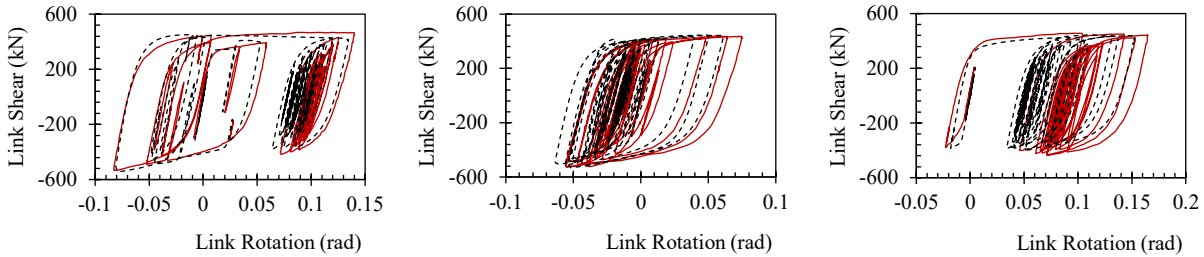


Figure 12: Second-Floor Link Hysteretic Responses from Hybrid Simulations on the Two-Story Industrial Compound

## CONCLUDING REMARKS

This paper provides a summary of a set of pseudo-dynamic hybrid simulations on two reference buildings designed with EBFs, which are equipped with the recently proposed cast steel replaceable modular yielding links. The study also provides a framework for performing hybrid simulations on EBFs, where the response of the yielding link is captured physically in an SDOF control system with or without axial loads. In hybrid simulations on the four-story EBF, the response of the first-floor link is captured physically, while the response of the rest of the structure is modelled numerically in OpenSees. The four-story building was designed such that the yielding links experience no axial loads. In hybrid simulations on the two-story EBF, the response of the roof level yielding link is captured physically, while the response of the rest of the structure is captured numerically. Given the EBF configuration and the distribution of the seismic mass with respect to the EBF, the roof level yielding links experience large axial loads in conjunction with their shear load and bending moments. Therefore, the experimental test setup was designed to impose the same level of axial load on the yielding link at the roof level. The study leads to the following conclusions.

- Results from the hybrid simulations demonstrate the effectiveness of the proposed framework for hybrid simulation on EBFs, with or without axial loads.
- In hybrid simulations where the yielding links are subjected to significant axial loads, maintaining a consistent  $P_{Link}/V_{Link}$  ratio in the experimental setup allows for capturing the yielding link's response using a single DOF control system.
- The EBFs designed with cast steel links demonstrated a satisfactory performance and sustained three MCE-level earthquakes without any indication of deterioration in strength or stiffness. The performance of the EBFs during the MCE-level seismic events was in line with MCE-level demands. In the four-story reference structure, the EBF100 experienced maximum rotations of 0.12, 0.11, and 0.18 radians in HS-1, HS-2, and HS-3, respectively. Meanwhile, the EBF77 in the two-story building underwent maximum rotations of 0.14, 0.08, and 0.17 radians in HSF-4, HSF-5, and HSF-6, respectively. Although the intensity of the response under individual seismic records differed depending

on the building's period and the frequency content of the motion, the observed range of link rotations in the hybrid simulations was consistent with anticipated link rotations for yielding links in EBFs during MCE-level seismic events.

- The experimental results highlight that significant residual rotations occur in EBF yielding links, even when residual drifts are moderate. This is due to the concentration of inelastic deformations at the link location, which is the intended mechanism in EBFs.
- Application of replaceable links in EBFs is intended to facilitate a simplified repair process after a major earthquake by replacing the damaged yielding link. However, large residual rotations may impede this repair process. Therefore, further research on the mitigation of residual rotations in EBFs is recommended, especially when replaceable yielding links are used in the design.

## ACKNOWLEDGMENTS

The authors acknowledge the support of the Natural Sciences and Engineering Research Council of Canada (NSERC) [ALLRP 560261-20] and Ontario Centres of Excellence (OCE VIP II-27058).

## REFERENCES

- [1] Fujimoto, M., Aoyagi, T., Ukai, K., Wada, A., Saito, K. (1972). "Structural characteristics of eccentric k-braced frames" *Transactions Architectural Institute of Japan*.
- [2] Popov, P., Takanashi, K., Roeder, C. (1976). "Structural steel bracing systems: behavior under cyclic loading", Report No. EERC 76-17, *Earthquake Engineering Research Institute*.
- [3] Roeder, CW., Popov, EP. (1977). "Inelastic behavior of eccentrically braced steel frames under cyclic loading", *UCB/EERC-17/18*, University of California Berkeley.
- [4] Hjelmstad, KD., Popov, EP. (1983). "Cyclic behavior and design of link beams", *ASCE Journal of Structural Engineering*, 109 (10) (1983), pp. 2387-2403.
- [5] Malley, JO., Popov, EP. (1984). "Shear links in eccentrically braced frames", *ASCE Journal of Structural Engineering*, 110 (9) (1984), pp. 2275-2295.
- [6] Kasai, K., Popov, EP. (1986). "General behavior of WF steel shear link beams", *ASCE Journal of Structural Engineering*, 112 (2) (1986), pp. 362-382.
- [7] Engelhardt, MD., Popov, EP. (1989). "On design of eccentrically braced frames" *Earthquake Spectra*. 5(3): 495-511.
- [8] Engelhardt, MD., Popov, EP. (1992). "Experimental performance of long links in eccentrically braced frames." *ASCE Journal of Structural Engineering*. 118(11): 3067-3088.
- [9] Okazaki, T., Arce, G., Ryu, HC., Engelhardt, MD. (2005). "Experimental study of local buckling, overstrength, and fracture of links in eccentrically braced frames." *ASCE Journal of Structural Engineering*. 131:1526-1535.
- [10] Okazaki, T., Engelhardt, MD. (2007). "Cyclic loading behavior of EBF links constructed of ASTM A992 steel" *Journal of Construction Steel Research*. 63(6): 751-765.
- [11] Berman, JW., Bruneau, M. (2007). "Experimental and analytical investigation of tubular links for eccentrically braced frames" *Engineering Structures*. 29(8): 1929-1938.
- [12] Mansour, N., Christopoulos, C., Tremblay, R. (2011). "Experimental validation of replaceable shear links for eccentrically braced steel frames" *ASCE Journal of Structural Engineering*. 137(10): 1141-1152.
- [13] Itani, AM., Elfass, S., Douglas, BM. (2003). "Behavior of built-up shear links under large cyclic displacement" *Engineering Journal*. 40(4): 221-234.
- [14] AISC (American Institute of Steel Construction). (2016). "Seismic provisions for structural steel buildings". AISC 341-16. Chicago, IL: AISC.
- [15] CSA S16 (Canadian Standard Association). (2019). "Design of Steel Structures". CSA S16-19, Toronto, Canada.
- [16] Bruneau, M., MacRae, G. (2017). "Reconstructing Christchurch: A seismic shift in building structural systems" *The Quake Centre*, University of Canterbury.
- [17] Martyr, R., Christopoulos, C. (2018). "Applying the cyclic void growth model to assess the ultralow cycle fatigue life of steel casting" *ASCE Journal of Structural Engineering*. 144 (8): 04018129.
- [18] Zhong, C., Binder, J., Kwon, O., Christopoulos, C. (2020). "Experimental and numerical characterization of ultralow-cycle fatigue behavior of steel casting." *ASCE Journal of Structural Engineering*. 146(2): 04019195.
- [19] Mortazavi, P., Kwon, O., Christopoulos, C. (2022). "Four-Element Pseudodynamic Hybrid Simulation of a Steel Frame with Cast Steel Yielding Connectors under Earthquake Excitations" *ASCE Journal of Structural Engineering*. 148 (2).
- [20] Lomax, K. B. (1982). "Forging and castings." *Materials for the process industrie: papers originally prepared for a conference held in 1982*, (pp. 23-24). London: Mechanical Engineering Publications.
- [21] Armitage, R. (1983). "Development of cast node joints for offshore production platforms." *Solidification technology in the foundry and cast house*. (pp. 385-391). London: The Metals Society.

- [22] Tan, K., Christopoulos, C. (2016). "Development of replaceable cast steel links for eccentrically braced frames." ASCE Journal of Structural Engineering. 142 (10): 04016079.
- [23] Mortazavi, P., Lee, E., Binder, J., Gray, M., Kwon, O., Christopoulos, C. (2020). "Overview of an experimental program on cast-steel replaceable yielding links in eccentrically braced frames" 17 World Conference on Earthquake Eng., Sendai, Japan.
- [24] Mortazavi, P., Lee, E., Binder, J., Kwon, O., Christopoulos, C. (2023). "Large-Scale Experimental Validation of Optimized Cast Steel Replaceable Modular Yielding Links for Eccentrically Braced Frames" ASCE Journal of Structural Engineering.
- [25] Mortazavi, P., Binder, J., Kwon, O., Christopoulos, C. (2023). "Ductility-Targeted Design of Cast Steel Replaceable Modular Yielding Links and their Experimental Validation through Large-Scale Testing" ASCE Journal of Structural Engineering.
- [26] Mortazavi, P., Binder, J., Kwon, O., Christopoulos, C. (2023). "Experimental Validation of Optimized Cast Steel Replaceable Modular Yielding Links for use in Eccentrically Braced Frames" Canadian Conference – Pacific Conference on Earthquake Engineering 2023, Paper No. 22, Vancouver, BC, Canada.
- [27] Maison, B. F., and Speicher, M. S. (2016). "Loading protocols for ASCE 41 backbone curves." Earthquake Spectra, 32(4), 2513- 2532
- [28] Suzuki, Y., and Lignos, D. G. (2020). "Development of collapse-consistent loading protocols for experimental testing of steel columns." Earthquake Engineering & Structural Dynamics, 49(2), 114-131.
- [29] Mojiri, S., Mortazavi, P., Kwon, O., Christopoulos, C. (2021). "Seismic response evaluation of a 5-story buckling restrained braced frame using multi-element pseudo-dynamic hybrid simulations." Earthquake Engineering and Structural Dynamics. <https://doi.org/10.1002/eqe.3508>
- [30] Mortazavi, P., Mojiri, S., Kwon, O., Christopoulos, C. (2022). "Multielement hybrid Simulations for Performance Assessment of Multistory Special Concentrically Braced Frames." ASCE journal of Structural Engineering, 148(9). [https://doi.org/10.1061/\(ASCE\)ST.1943-541X.0003439](https://doi.org/10.1061/(ASCE)ST.1943-541X.0003439)
- [31] American Society of Civil Engineers (ASCE), "Minimum design loads for buildings and other structures", ASCE/SEI 7-10, Including supplement No.1. Reston, VA.: American Society of Civil Engineers, 2016.
- [32] American Institute of Steel Construction (AISC), "Load and resistance factor design specification for structural steel buildings", ANSI/AISC 360-16 Including supplement No.1. Chicago: American Institute of Steel Construction, Inc, 2016.
- [33] American Institute of Steel Construction (AISC), "Seismic provisions for structural steel buildings", ANSI/AISC 341-16 Including supplement No.1. Chicago: American Institute of Steel Construction, Inc, 2016
- [34] Mortazavi, P., Kwon, O., Christopoulos, C. (2023). "Pseudo-dynamic hybrid simulations of steel eccentrically braced frames equipped with cast steel replaceable modular yielding links". *Earthquake Engineering and Structural Dynamics*.
- [35] Mortazavi, P. (2023). "Large-Scale Experimental Validation and Design of Resilient EBFs with Cast Steel Replaceable Modular Yielding Links", PhD Dissertation, University of Toronto.
- [36] PEER Ground Motion database. Pacific Earthquake Engineering Research Center. <http://ngawest2.berkeley.edu> [26 August 2015]
- [37] Combescure D. Pegon P. (1997). "α-Operator splitting time integration technique for pseudodynamic testing error propagation analysis" Soil Dynamics and Earthquake Engineering. 16 (7– 8): 427–443. DOI: 10.1016/S0267-7261(97)00017-1.
- [38] Huang X, Kwon O. (2020). "A generalized numerical/experimental distributed simulation framework" Journal of Earthquake Engineering. Jan 11:1-22. DOI: 10.1080/13632469.2018.1423585
- [39] Mortazavi P, Huang X, Kwon O, Christopoulos C. (2017). "Example manual for University of Toronto Simulation (UT-SIM) Framework. An open-source framework for integrated multi-platform simulations for structural resilience (Second edition)", Technical Report, International Workshop on Hybrid Simulation, Department of Civil Engineering, University of Toronto, Canada, 2017.
- [40] Mortazavi P, Huang X, Kwon O, Christopoulos C. (2017). "An overview of the University of Toronto Simulation (UT-SIM) Framework and its application to the performance assessment of structures", Proceedings of the 7th Int. Conference on Advances in Experimental Structural Engineering, Pavia, Italy, 2017.
- [41] Zhan, H., Kwon, O. (2015). "Actuator controller interface program for pseudo-dynamic hybrid simulation". *The 2015 World Congress on Advances in Structural Engineering and Mechanics*, Incheon, Korea, August 25-29, 2015.
- [42] Huang, X., Park, J., and Kwon, O. (Accepted). "Network Interface Program for Actuator Controllers for Pseudo-Dynamic Hybrid Simulation," Journal of Earthquake Engineering, DOI:10.1080/13632469.2023.2197501
- [43] National Instruments. <http://www.ni.com> [1 September 2015].
- [44] MTS Flextest models 40/60/100/200 controller hardware, User's manual.